JFM RAPIDS
journals.cambridge.org/rapids

Network structure of two-dimensional decaying isotropic turbulence

Kunihiko Taira[1],†, Aditya G. Nair[1] and Steven L. Brunton[2]

[1]Department of Mechanical Engineering, Florida State University, Tallahassee, FL 32310, USA

[2]Department of Mechanical Engineering, University of Washington, Seattle, WA 98195, USA

The present paper reports on our effort to characterize vortical interactions in complex fluid flows through the use of network analysis. In particular, we examine the vortex interactions in two-dimensional decaying isotropic turbulence and find that the vortical-interaction network can be characterized by a weighted scale-free network. It is found that the turbulent flow network retains its scale-free behaviour until the characteristic value of circulation reaches a critical value. Furthermore, we show that the two-dimensional turbulence network is resilient against random perturbations, but can be greatly influenced when forcing is focused towards the vortical structures, which are categorized as network hubs. These findings can serve as a network-analytic foundation to examine complex geophysical and thin-film flows and take advantage of the rapidly growing field of network theory, which complements ongoing turbulence research based on vortex dynamics, hydrodynamic stability, and statistics. While additional work is essential to extend the mathematical tools from network analysis to extract deeper physical insights of turbulence, an understanding of turbulence based on the interaction-based network-theoretic framework presents a promising alternative in turbulence modelling and control efforts.

1. Introduction

Recent advances in the field of network analysis have revealed the structures of internet, technological, social and biological networks (Albert & Barabási 2002; Newman 2003, 2010; Barrat *et al.* 2004*a*). Having characterized these networks, we are able to study dynamics such as disease outbreak and information propagation on networks, and analyse the resilience of network-based activities (Albert, Jeong & Barabási 2000; Barrat, Barthélemy & Vespignani 2008). These analysis techniques are founded on graph theory, dynamical systems, and operator theory, but place unique

† Email address for correspondence: ktaira@fsu.edu

emphasis on interactions and connectivity amongst the elements that establish a network. Thus far, most of the applications of network analysis have been concerned with discrete settings in which nodes are individualized quantities, such as people, organisms, equipment, or stations (Caldarelli 2007; Newman 2010). In this paper, we extend the network analysis to continuous representation of physical phenomena, in particular two-dimensional turbulence.

The chaotic motion of a large number of vortices in turbulent flows is caused by the induced velocities of the vortices themselves. What makes turbulence rich and complex are the vortical interactions in the flow field, which take place over a wide range of length scales (Tennekes & Lumley 1972; Hinze 1975; Frisch 1995; Pope 2000; Davidson 2004; Lesieur 2008). Thus, complete understanding of turbulence has remained a challenge to this day because of its high-dimensionality, multiscale interactions, nonlinearity and the resulting chaos. Network science provides an alternative view of complex fluid flows in terms of a network of vortex interactions (Nair & Taira 2015), and this perspective illuminates the underlying structure and organization of turbulent flows. In this work, we show that two-dimensional isotropic turbulence (Kraichnan & Montgomery 1980; McWilliams 1984; Benzi, Paladin & Vulpiani 1990; Benzi & Colella 1992; Davidson 2004; Boffetta & Ecke 2012) has a scale-free network structure reminiscent of other networks found in nature (Barabási & Albert 1999; Caldarelli 2007). While most of the attention has been placed on unweighted scale-free networks, we consider the use of weighted scale-free networks to describe the variations in the strength of interactions or connectivities (Barrat, Barthélemy & Vespignani 2004b). Upon identifying the network structure of turbulence, physical insights can be obtained as to which vortical interactions are important in capturing the overall physics and how it may be possible to control the dynamics of turbulent vortices (Farazmand, Kevlahan & Protas 2011; Liu, Slotine & Barabási 2011; Brunton & Noack 2015).

2. Problem description and approach

To extract the network structure of the flow, we quantify the interactions between fluid elements based on the vortical interactions. The velocity $\boldsymbol{u}$ at position $\boldsymbol{x}$ induced by the vorticity distribution $\boldsymbol{\omega}$ of the flow is

$$\boldsymbol{u}(\boldsymbol{x}, t) = \frac{1}{4\pi} \int \frac{\boldsymbol{\omega}(\tilde{\boldsymbol{x}}, t) \times (\boldsymbol{x} - \tilde{\boldsymbol{x}})}{|\boldsymbol{x} - \tilde{\boldsymbol{x}}|^3} \, \mathrm{d}\tilde{\boldsymbol{x}}. \quad (2.1)$$

In this study, we focus on unforced two-dimensional isotropic turbulence in a periodic box and assess the influence of the vorticity distribution over a Cartesian domain. Here, the two-dimensional vorticity field reduces to $\boldsymbol{\omega}(\boldsymbol{x}, t) = \omega(x, y, t)\hat{\boldsymbol{e}}_z$, with $\hat{\boldsymbol{e}}_z$ denoting the unit normal plane vector. Modelling the vortical component for each discrete Cartesian element as a line vortex, we can evaluate how fluid elements influence each other, as depicted in figure 1. Here, the magnitude of the induced velocity from fluid element i on another element j reduces from (2.1) to

$$u_{i \to j} = \frac{|\gamma_i|}{2\pi |\boldsymbol{x}_i - \boldsymbol{x}_j|}, \quad (2.2)$$

where $\gamma_i = \omega(\boldsymbol{x}_i)\Delta x \Delta y$ is the circulation of fluid element i with side lengths of Δx and Δy. The superposition of the induced velocity from all other fluid elements provides the advective velocity of the fluid element. Detailed discussions on using point vortices to develop the network-theoretic framework for describing unsteady vortical flows can
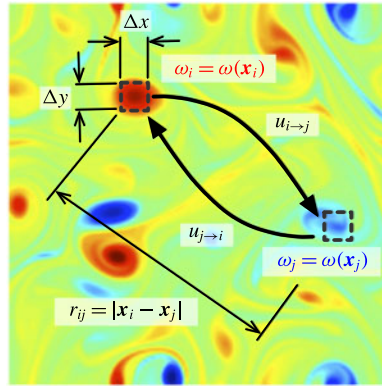
FIGURE 1. Interaction of fluid elements in two-dimensional turbulence. The strength of the vortical interaction between elements i and j having vorticity ω_i and ω_j is quantified through the induced velocities $u_{i \to j}$ and $u_{j \to i}$, respectively. For discretizing the Cartesian domain, we take n_x and n_y points in the horizontal and vertical directions, respectively, providing the adjacency matrix $\boldsymbol{A}$ of size $n \times n$ with $n = n_x n_y$. Shown in the background with a contour plot is the corresponding vorticity field with initial $Re(t_0) = 814$ at $t = 18$.

be found in Nair & Taira (2015). Note that adjacency matrices are commonly defined with positive weights as considered here, but they can be relaxed to accommodate positive and negative weights within the context of vortical interactions. This point will be revisited later.

To assess and describe the vortical interactions in the flow field, we utilize a weighted network (graph). The definition of a network (graph) $\mathscr{G}$ requires sets of vertices (nodes) $\mathscr{V}$, edges $\mathscr{E}$, and weights $\mathscr{W}$ (Newman 2010). With these three components defined, a graph can be uniquely determined, i.e. $\mathscr{G} = \mathscr{G}(\mathscr{V}, \mathscr{E}, \mathscr{W})$. The nodes $\mathscr{V}$ in this study are taken to be the vortical elements residing within the Cartesian cells, while the edges $\mathscr{E}$ represent the vortical interactions between those vortical elements. The edge weights $\mathscr{W}$ quantify the strengths of the vortical interactions. Given n nodes, a collection of the weights w_{ij} in the form of a matrix $\boldsymbol{A} \in \mathbb{R}^{n \times n}$ with

$$A_{ij} = \begin{cases} w_{ij} & \text{if } (i, j) \in \mathscr{E} \\ 0 & \text{otherwise,} \end{cases} \tag{2.3}$$

is called the adjacency matrix and is used to describe the network connectivity. In the above definition, A_{ij} is set to the edge weight w_{ij} if there exists an edge (interaction) between nodes i and j. Details on the fundamental concepts involved in network theory can be found in Dorogovtsev (2010) and Newman (2010), with descriptions of vortical-interaction networks in Nair & Taira (2015).

Based on (2.2), we define the network adjacency matrix as the average induced velocity

$$A_{ij} = \begin{cases} \frac{1}{2}(u_{i \to j} + u_{j \to i}) & \text{if } i \neq j \\ 0 & \text{otherwise} \end{cases} \tag{2.4}$$

to quantify the magnitude of interaction between fluid elements i and j (Nair & Taira 2015). Note that an element cannot impose velocity upon itself, which is captured by the null entry along the diagonal of the adjacency matrix. In the present study, the

influence from the neighbouring periodic vortex images are also accounted for in the analysis. This formulation yields a full matrix, except for its diagonal entries, which are identically zero. In assessing the strength of the vortical interaction between two fluid elements, we utilize (2.4) to perform network analysis to extract the spatial connectivity structure. This approach has been successful in capturing the nonlinear vortex dynamics and modelling the trajectories of vortex clusters (Nair & Taira 2015). The adjacency matrix considered here is symmetric to quantify the average interaction strength. Note that the geometric mean can be alternatively chosen and yields similar results. In general, the adjacency matrix can be formulated in an asymmetric manner:

$$A_{ij} = \begin{cases} \phi u_{i \to j} + (1 - \phi) u_{j \to i} & \text{if } i \neq j \\ 0 & \text{otherwise.} \end{cases} \tag{2.5}$$

Here the parameter ϕ takes a value between 0 and 1. For the aforementioned symmetric formulation in (2.4), ϕ is selected as $1/2$. When $\phi = 0$ and 1, the adjacency matrix A_{ij} are defined by the velocity imposed to the other elements ($A_{ij} = u_{j \to i}$) and upon themselves ($A_{ij} = u_{i \to j}$), respectively, for $i \neq j$. We mainly focus on the use of the symmetric adjacency matrix in this work, but will consider the asymmetric formulation briefly to highlight the difference from a physical point of view in the next section. We note in passing that the theoretical tools for symmetric adjacency matrices are more widely available compared to the asymmetric matrices.

The flow field analysed in this study is obtained from direct numerical simulation on a square biperiodic computational domain $(x, y) \in [0, L] \times [0, L]$ with a grid size of $m_x \times m_y = 1024 \times 1024$. The unforced two-dimensional incompressible isotropic turbulent flow is simulated by numerically solving the two-dimensional vorticity transport equation

$$\frac{\partial \omega}{\partial t} + u_j \frac{\partial \omega}{\partial x_j} = \frac{1}{Re} \frac{\partial^2 \omega}{\partial x_j \partial x_j}, \tag{2.6}$$

where $\boldsymbol{u}$ and ω are the velocity and vorticity variables, respectively. The simulation is performed with the Fourier spectral method and the fourth-order Runge–Kutta time integration scheme (Canuto *et al.* 1988). The vorticity field is initialized with a smooth distribution comprised of a large number (≈ 100) of superposed vortices (Taylor 1918) with random strengths, core sizes, and locations chosen such that the kinetic energy spectra satisfies $E(k) \propto k \exp(-k^2/k_0^2)$, where $k_0 = 26.5$, following the set-up by Kida (1985) and Brachet, Meneguzzi & Sulem (1986). The initial core sizes are selected to be sufficiently small compared to the size of the computational domain (McWilliams 1984) arranged in random positions. The velocity variable is normalized by the square root of the spatial average of the initial kinetic energy $u^*(t_0) \equiv [\overline{u^2(t_0)}]^{1/2}$, where the overline denotes the spatial average. The spatial length and time scales are non-dimensionalized by the initial integral length scale $l^*(t_0) \equiv [2\overline{u^2(t_0)}/\overline{\omega^2(t_0)}]^{1/2}$ and the initial eddy turnover time $t_0^* \equiv l^*(t_0)/u^*(t_0)$, respectively. The Reynolds number is defined accordingly as $Re \equiv u^* l^*/\nu$, where ν is the kinematic viscosity. In this study, turbulent flows with initial Reynolds numbers of $Re(t_0) = 75, 439, 814, 1607$ and 2485 are selected.

3. Results

3.1. *Network-based characterization*

We identify the underlying network structure and characteristics of two-dimensional turbulence based on the aforementioned symmetric adjacency weights. The time-evolving vorticity field is obtained from a two-dimensional incompressible biperiodic

direct numerical simulation (Canuto *et al.* 1988) for unforced isotropic turbulence. Given the vorticity field over a Cartesian grid, each fluid element is considered to be connected to all other elements through vortical network edges. The resulting fluid flow network can in fact be described by a complete graph with a range of weights. Next, we visualize the network edges with a transparent grey scale corresponding to the adjacency weight, as shown in figure 2(*a*). The captured structure reveals the turbulent network. Some regions in the flow have a large number of strong connections, corresponding to larger stronger vortices seen in red, serving as primary network hubs. Note that these strong vortices induce velocities over long distances. Moderate size vortices that act as secondary hubs also possess dominant connections to primary hubs and other secondary hubs. In contrast, fluid elements corresponding to smaller, weaker eddies, shown in blue, generally have influence only in their vicinity. The node strength distribution ($s_i = \sum_j A_{ij}$) over space shows that the vortices with large circulation have larger strength, as illustrated in figure 2(*b*). The node strength distribution over space enables us to distinguish secondary and primary hubs, which may not be easily differentiated from simply visualizing the vorticity field or the Q criterion in a traditional manner. For instance, see the green vortices in figure 2(*b*), which can appear similar to primary ones in vorticity level.

Plotting the probability of the strength distribution $P(s)$ over the strength s of fluid elements in figure 2(*c*), we find that two-dimensional isotropic turbulence network has a power-law distribution $P(s) \sim s^{-\gamma}$, with $\gamma = 2.7$, at the time shown. This tells us that the vortex interactions in turbulence can be characterized by a weighted scale-free network. This realization enables the interaction-based analysis of turbulent flows from a new perspective through network theory (Cohen & Havlin 2010; Newman 2010). In particular, this type of network is known to have certain resilience properties, as we will explore later in this section. Also shown in figure 2(*c*) in grey are the degree distributions for asymmetric adjacency formulations. The out- and in-degree distributions can be found by setting $\phi = 0$ and 1, respectively, in (2.5). It can be observed that the scale-free symmetric distribution is mostly comprised of the out-degree components, which describe how each vortical element influences all other elements (i.e. $u_{j \to i}$). In contrast, we find that the in-degree distribution has a single peak, which conveys that all fluid elements receive a similar amount of collective influence from vortices in the flow field. We have found that the scale-free property of two-dimensional isotropic turbulence is most well captured by the symmetric weights compared to the other asymmetric formulations. It is also possible to examine the strength distribution taking positive and negative values of circulations, as we have briefly discussed in § 2. Utilizing positive and negative weights, their strength distribution can also exhibit a scale-free behaviour, but with network strength having both negative and positive values. This leads to a symmetric strength distribution over the strength, with a resemblance to the probability density function of scaled displacements (Weiss, Provenzale & McWilliams 1998). In what follows, results based on the symmetric adjacency matrix (using the magnitude of induced velocity) are presented.

Let us further examine the time-varying properties of the turbulent network. In unforced turbulence, the kinetic energy of the flow decreases over time due to viscous dissipation, as shown in figure 3(*a*). The strength distribution $P(s)$ of the turbulence network and the corresponding flow field snapshots are presented in figure 3(*b*). Turbulent flow is comprised of vortical structures over a wide range of spatial scales initially. The distribution $P(s)$ exhibits scale-free characteristics with $P(s) \sim s^{-\gamma}$, where $\gamma \approx 2.7$, when the kinetic energy spectra exhibits the k^{-3} profile for $t \lesssim 30$. For the
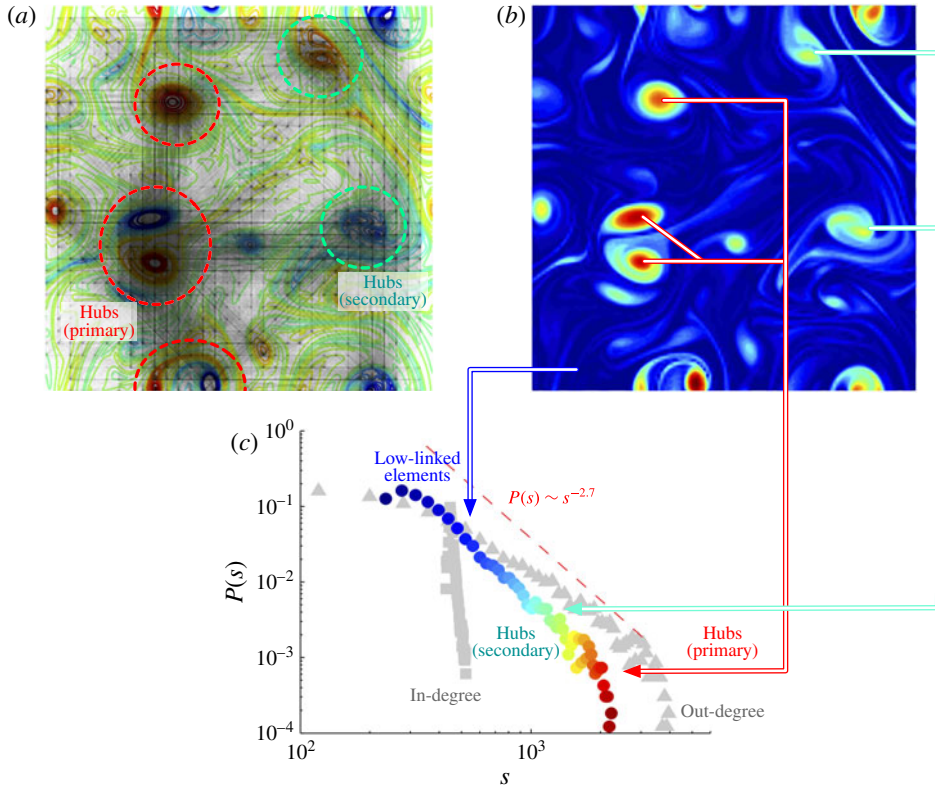
FIGURE 2. The scale-free network of vortical interactions in two-dimensional turbulence with initial $Re(t_0) = 814$. (*a*) Turbulent network structure overlaid on the vorticity field, with the darkness of the network edges corresponding to the values of the adjacency weights ($t = 18$). (*b*) Contour plot of the node strength s distribution. Vortex cores having high degree of connectivity act as hubs in the turbulent vortical network. (*c*) The corresponding node strength probability distribution, exhibiting the scale-free characteristics with $P \sim s^{-2.7}$. The same contour level is shared by (*b,c*). Also shown in the background of (*c*) in grey are the out and in-degree distributions ($\phi = 0$ and 1, respectively). The network visualized in (*a*) does not show interactions from periodic images, and uses 32×32 nodes for graphical clarity.

flow under consideration, a bend in the strength distribution appears for $t \gtrsim 30$ as the system starts to exhibit scale separation and loses the k^{-3} energy spectra. This is caused by the diffusion of smaller-scale structures and their merging with other structures. Over time, viscous dissipation removes kinetic energy through the smaller eddies and leaves only the larger vortices. This behaviour can be described by two power laws, $P(s) \sim s^{-\gamma_1}$ and $P(s) \sim s^{-\gamma_2}$, which capture the weaker fluid elements and the larger stronger vortices, respectively. The bifurcation of these power laws is shown in figure 3(*c*), indicated by the vertical dashed line. We note that, regardless of the initial condition used, the turbulent interaction network maintains the scale-free behaviour in the present investigation as long as the energy spectra relaxes to the k^{-3} profile (Kida 1985; Brachet *et al.* 1986; Benzi *et al.* 1990). This scale-free behaviour may be observed during the initial transient, but is not a guaranteed common feature without the k^{-3} energy spectra being present.
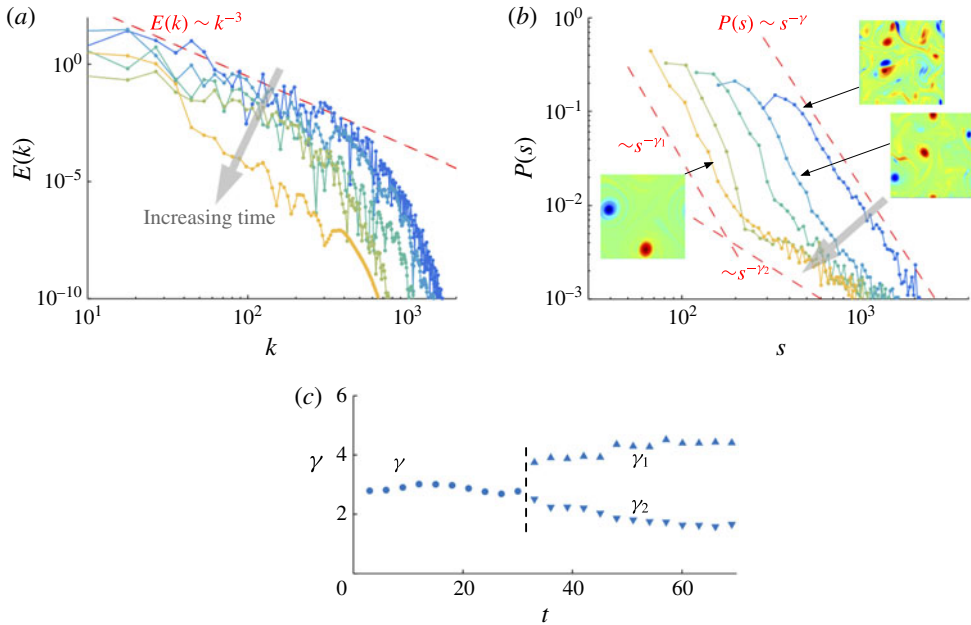
795 R2-6

FIGURE 3. The dynamics of a turbulent network with $Re(t_0) = 814$. (*a*) Kinetic energy and (*b*) strength distribution of two-dimensional isotropic turbulence for $t = 15$, 30, 75, 150 and 300 (line colours represent time). The inset plots in (*b*) show the corresponding vorticity fields. The kinetic energy $E(k)$ is shown over the wavenumber k, exhibiting the asymptotic profile of $E(k) \sim k^{-3}$. The strength distribution $P(s)$ displays the scale-free property of $P(s) \sim s^{-\gamma}$ over node strength s. (*c*) The corresponding exponents γ, γ_1 and γ_2 are shown. Later in time the strength distribution exhibits the emergence of two distributions, $P(s) \sim s^{-\gamma_1}$ and $s^{-\gamma_2}$.

We have considered a range of Reynolds numbers and observed that γ takes values of $\gamma = 2.7 \pm 0.5$. The variations observed in γ, γ_1 and γ_2 shown in figure 3(*c*) are influenced by the chaotic nature of turbulence. These parameters, however, appear to exhibit a coalescing behaviour when they are plotted over the product of the characteristic velocity and length, $u^*(t)l^*(t)$. Here, we interpret $u^*(t)l^*(t)$ as the circulation of vortices that have the characteristic velocity and length scales. As shown in figure 4, we observe that the turbulence network shows coalescence of the scale-free parameter γ to $\gamma_{cr} \approx 2.7$ over time for different cases of turbulent flows. Once the flows reach a state where the characteristic strength of vortices is $(u^*l^*)_{cr} \approx 0.063$, the network distribution bifurcates to display two different slopes with γ_1 and γ_2, as previously illustrated in figure 3. This observation reveals that a scale-free turbulent network is present until the unforced turbulent flow field loses the smaller-scale vortices, and mostly contains vortices with strengths larger than the critical value of $(u^*l^*)_{cr}$.

3.2. *Resilience of turbulence networks*

Characterizing turbulent flow with a scale-free network enables us to view turbulent interactions in a systematic manner, and provides insights into how vortical structures influence each other. It is known from network analysis that scale-free networks
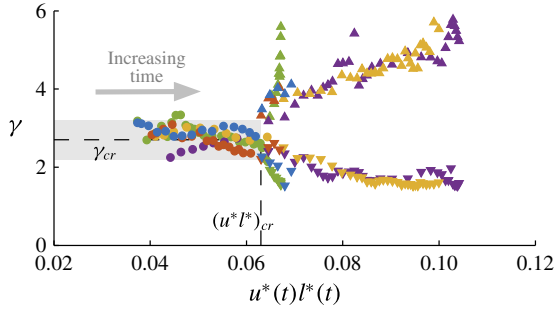
FIGURE 4. Exponent γ for the network strength distribution $P(s) \sim s^{-\gamma}$ plotted over $u^*(t)l^*(t)$ with different initial Reynolds numbers (green: $Re(t_0) = 75$, purple: $Re(t_0) = 439$, yellow: $Re(t_0) = 814$, red: $Re(t_0) = 1607$, and blue: $Re(t_0) = 2485$). Scale-free distributions are observed with γ coalescing to $\gamma_{cr} \approx 2.7$ up until a bifurcation at $(u^*l^*)_{cr} \approx 0.063$. The grey box shows $\gamma = 2.7 \pm 0.5$ as reference.

are resilient to random perturbations, but attacks towards network hubs can affect network dynamics in a detrimental manner (Albert *et al.* 2000). Network resilience for fluid flow translates to the difficulty of modifying the vortical-interaction network and, consequently, the collective behaviour of the vortices over time. To measure the change in vortical interaction caused by network disturbance, we can consider how the removal of turbulence network nodes (percolation) modifies the characteristic network length

$$l_{network} \equiv \frac{1}{n(n-1)} \sum_{i \neq j} \min d(i, j), \tag{3.1}$$

which is the average shortest network distance $d(i, j)$ between any two nodes on a network. Here, we perform node percolation by setting the vorticity values at the chosen nodes to be zero. The above metric quantifies how well vortical elements are connected within a turbulent network. Note that the distance here refers to network distance based on the adjacency matrix, and not the spatial distance. In particular, we take the inverse of each adjacency weight $1/a_{ij}$ and evaluate the minimal sum

$$d(i, j) = 1/a_{ik_1} + 1/a_{k_1 k_2} + \cdots + 1/a_{k_m j} \tag{3.2}$$

over a network path that connects nodes i and j for this metric (Rubinov & Sporns 2010). This metric $l_{network}$ can be thought of as the average of the minimal characteristic advective (commute) time per unit length between every pair of fluid elements in the domain. This minimal network distance is determined using the Floyd–Warshall algorithm (Floyd 1962).

The changes in the turbulence network characteristic length $l_{network}$ when network nodes are removed in a random fashion and a coordinated manner targeting hub nodes are summarized in figure 5. Here, the changes in the normalized characteristic network length

$$\Delta \tilde{l}_{network} \equiv \frac{l_{network}(t, f) - l_{network}(t, f = 0)}{l_{network}(t, f = 0)} \tag{3.3}$$

for varied fraction of node removal f are shown. While it would be difficult to completely remove nodes, as we have performed in this investigation, the present
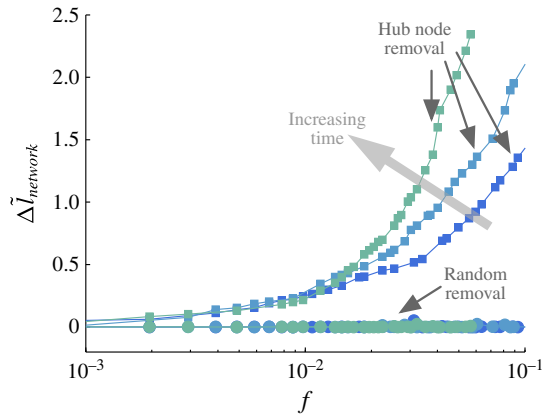
795 R2-8

FIGURE 5. The resilience of turbulence network against fraction of node removals, f, for $t = 15$, 30 and 75, with $Re(t_0) = 814$. Shown are relative changes in the characteristic network length $\Delta \tilde{l}_{network}$ of turbulent flow for random node and hub node removals. The colours of the curves represent the time when node removal is considered, and follows figure 3.

analysis sheds light on how external forcing or perturbations can alter the turbulent flow from an interaction-based analysis. We observe that turbulent flow is resilient against random forcing, as evident from the characteristic network length being unaffected even for a large fraction f of nodes being removed. This behaviour is consistently observed over time. On the other hand, we find that the global vortical-interaction network can be greatly modified by targeting large vortex cores (hubs), as exhibited by the substantial change in the characteristic length. It may be more energetically expensive to remove well-connected hub nodes, which often correspond to regions of concentrated vorticity. However, it is clear from figure 5 that even the smallest fraction of hub node removal can influence the overall interaction, which suggests that hub removal still provides a more effective and efficient way to modify the flow than random node removal.

When the vortical-interaction network is grossly altered, the dynamics of the collection of vortices would be significantly modified (Nair & Taira 2015). These observations also agree with past studies in flow control that identified effective actuation frequencies to be associated with the length scale of the large coherent structures in turbulent flows (Gad-el-Hak 2000; Joslin & Miller 2009). With increasing time, we can further notice that network connectivity decreases with hub removal, due to viscous dissipation of smaller vortical structures, and the influence of removing the core structures becomes more evident. The present network-based understanding reveals which types of flow structure should be targeted with flow control if we aim to alter the behaviour of the turbulent flow field in a global manner.

4. Concluding remarks

The approach presented in this paper is the initial effort in performing network-based analysis of complex turbulent flows. Using the mathematical toolsets from network theory, we have identified that the vortical interactions in two-dimensional decaying isotropic turbulence have a scale-free network structure. We have been able to reveal the structure by taking a continuous representation of the flow field

and quantifying the network using a Cartesian discretization. For two-dimensional isotropic turbulence, the node strength distribution was uncovered to be $P(s) \sim s^{-\gamma}$, where $\gamma = 2.7 \pm 0.5$. Furthermore, we have found that the unforced turbulent flow field possesses an underlying scale-free network structure until the circulation of vortices with characteristic velocity and length scales reach $(u^*l^*)_{cr} \approx 0.063$. By noticing that the turbulence network has scale-free characteristics, we were able to systematically show that the turbulence network is resilient against random perturbations, but vulnerable against coordinated forcing on the hub vortices. It should be noted that estimating and controlling each and every vortical structure in a turbulent flow is most likely improbable and impractical. Instead, network analysis may provide a refreshing view point on how one can predict and modify the collective dynamics of vortices in the turbulent flow fields. We believe that network-based analysis and control (Mesbahi & Egerstedt 2010; Liu *et al.* 2011; Cornelius, Kath & Motter 2013; Kaiser *et al.* 2014; Yan *et al.* 2015) will provide a novel mathematical fabric for paving the path towards network-based modelling and control of turbulent flows, which can potentially impact a wide spectrum of problems.

Acknowledgements

References

ALBERT, R. & BARABÁSI, A.-L. 2002 Statistical mechanics of complex networks. *Rev. Mod. Phys.* **74** (1), 47–97.

ALBERT, R., JEONG, H. & BARABÁSI, A.-L. 2000 Error and attack tolerance of complex networks. *Nature* **406**, 378–382.

BARABÁSI, A.-L. & ALBERT, R. 1999 Emergence of scaling in random networks. *Science* **286**, 509–512.

BARRAT, A., BARTHÉLEMY, M., PASTOR-SATORRAS, R. & VESPIGNANI, A. 2004*a* The architecture of complex weighted networks. *Proc. Natl Acad. Sci. USA* **101** (11), 3747–3752.

BARRAT, A., BARTHÉLEMY, M. & VESPIGNANI, A. 2004*b* Weighted evolving networks: coupling topology and weighted dynamics. *Phys. Rev. Lett.* **92** (22), 228701.

BARRAT, A., BARTHÉLEMY, M. & VESPIGNANI, A. 2008 *Dynamical Processes on Complex Networks.* Cambridge University Press.

BENZI, R. & COLELLA, M. 1992 A simple point vortex model for two-dimensional decaying turbulence. *Phys. Fluids* A **4** (5), 1036–1039.

BENZI, R., PALADIN, G. & VULPIANI, A. 1990 Power spectra in two-dimensional turbulence. *Phys. Rev.* A **42** (6), 3654–3656.

BOFFETTA, G. & ECKE, R. E. 2012 Two-dimensional turbulence. *Annu. Rev. Fluid Mech.* **44**, 427–451.

BRACHET, M. E., MENEGUZZI, M. & SULEM, P. L. 1986 Small-scale dynamics of high-Reynolds-number two-dimensional turbulence. *Phys. Rev. Lett.* **57** (6), 683–686.

BRUNTON, S. L. & NOACK, B. R. 2015 Closed-loop turbulence control: progress and challenges. *Appl. Mech. Rev.* **67** (5), 050801.

CALDARELLI, G. 2007 *Scale-Free Networks.* Oxford University Press.

CANUTO, C., HUSSAINI, M. Y., QUARTERONI, A. & ZANG, T. A. 1988 *Spectral Methods in Fluid Dynamics.* Springer.

COHEN, R. & HAVLIN, S. 2010 *Complex Networks: Structure, Robustness and Function*. Cambridge University Press.

CORNELIUS, S. P., KATH, W. K. & MOTTER, A. E. 2013 Realistic control of network dynamics. *Nat. Commun* **4**, 1942.

DAVIDSON, P. A. 2004 *Turbulence: An Introduction for Scientists and Engineers*. Oxford University Press.

DOROGOVTSEV, S. N. 2010 *Lectures on Complex Networks*. Oxford University Press.

FARAZMAND, M. M., KEVLAHAN, N. K.-R. & PROTAS, B. 2011 Controlling the dual cascade of two-dimensional turbulence. *J. Fluid Mech.* **668**, 202–222.

FLOYD, R. W. 1962 Algorithm 97: shortest path. *Comm. ACM* **5** (6), 345.

FRISCH, U. 1995 *Turbulence*. Cambridge University Press.

GAD-EL-HAK, M. 2000 *Flow Control: Passive, Active, and Reactive Flow Management*. Cambridge University Press.

HINZE, J. O. 1975 *Turbulence*. McGraw-Hill.

JOSLIN, R. D. & MILLER, D. N. (Eds) 2009 *Fundamentals and Applications of Modern Flow Control*, AIAA.

KAISER, E., NOACK, B. R., CORDIER, L., SPOHN, A., SEGOND, M., ABEL, M., DAVILLER, G., OSTH, J., KRAJNOVIĆ, S. & NIVEN, R. K. 2014 Cluster-based reduced-order modelling of a mixing layer. *J. Fluid Mech.* **754**, 365–414.

KIDA, S. 1985 Numerical simulation of two-dimensional turbulence with high-symmetry. *J. Phys. Soc. Japan* **54** (8), 2840–2853.

KRAICHNAN, R. H. & MONTGOMERY, D. 1980 Two-dimensional turbulence. *Rep. Prog. Phys.* **43**, 547–619.

LESIEUR, M. 2008 *Turbulence in Fluids*, 4th edn. Springer.

LIU, Y.-Y., SLOTINE, J.-J. & BARABÁSI, A.-L. 2011 Controllability of complex networks. *Nature* **473** (7346), 167–173.

MCWILLIAMS, J. C. 1984 The emergence of isolated coherent vortices in turbulent flow. *J. Fluid Mech.* **146**, 21–43.

MESBAHI, M. & EGERSTEDT, M. 2010 *Graph Theoretic Methods in Multiagent Networks*. Princeton University Press.

NAIR, A. G. & TAIRA, K. 2015 Network-theoretic approach to sparsified discrete vortex dynamics. *J. Fluid Mech.* **768**, 549–571.

NEWMAN, M. E. J. 2003 The structural and function of complex networks. *SIAM Rev.* **45** (2), 167–256.

NEWMAN, M. E. J. 2010 *Networks: An Introduction*. Oxford University Press.

POPE, S. B. 2000 *Turbulent Flows*. Cambridge University Press.

RUBINOV, M. & SPORNS, O. 2010 Complex network measures of brain connectivity: uses and interpretations. *NeuroImage* **52**, 1059–1069.

TAYLOR, G. I. 1918 On the dissipation of eddies. Reports and Memoranda 598. Aero. Res. Comm.

TENNEKES, H. & LUMLEY, J. L. 1972 *A First Course in Turbulence*. MIT Press.

WEISS, J. B., PROVENZALE, A. & MCWILLIAMS, J. C. 1998 Lagrangian dynamics in high-dimensional point-vortex systems. *Phys. Fluids* **10** (8), 1929–1941.

YAN, G., TSEKENIS, G., BARZEL, B., SLOTINE, J.-J., LIU, Y.-Y. & BARABÁSI, A.-L. 2015 Spectrum of controlling and observing complex networks. *Nat. Phys* **11**, 779–786.